Journal of Sedimentary Research

Journal of Sedimentary Research, 2012, v. 82, 232–243
Research Article
DOI: 10.2110/jsr.2012.23

VERTICAL-TO-LATERAL TRANSITIONS AMONG CRETACEOUS CARBONATE FACIES—A MEANS TO 3-D FRAMEWORK CONSTRUCTION VIA MARKOV ANALYSIS

SAM PURKIS,[1] BRIGITTE VLASWINKEL,[2] AND NUNO GRACIAS[3]
[1]*National Coral Reef Institute, Nova Southeastern University, Dania Beach, Florida 33004, U.S.A.*
[2]*Shell International Exploration and Production, Rijswijk, 2288 GS, The Netherlands*
[3]*University of Girona, Girona, Spain*
e-mail: purkis@nova.edu

ABSTRACT: **The search for, and extraction of, hydrocarbons in carbonate rocks demands a thorough understanding of their depositional anatomy. The complexity of carbonate systems, however, hinders detailed direct characterization of their volumetric heterogeneity. Information with which to construct a reservoir model must therefore be based on information gathered from wells or outcrops transecting the sequence of interest. Most (particularly exploration wells) are vertical, presenting a problem for geostatistical modeling. While understanding vertical stratal stacking is straightforward, it is difficult to obtain lateral facies information. Though in some situations outcrop surfaces, seismic data, and horizontal wells may somewhat mitigate this bias, the likelihood remains that the lateral dimension of a buried system will be vastly undersampled with respect to the vertical. However, through the principle of Walther's Law (Walther 1894) or due to the geometry of basinward-inclined beds, comparable facies frequencies and transition probabilities may link vertical and lateral stratal arrangements, the implication being that a reservoir model, competent at least in terms of transition statistics, could be built against information harvested down-core. Taking an interpreted outcrop panel from Lewis Canyon (Albian, Pecos River, Texas), we use Markov-chains to first ascertain that vertical and lateral stratal ordering is nonrandom. Second, we show lithofacies transition probabilities in the outcrop as being interchangeable between the vertical and lateral directions. The work concludes by demonstrating the utility of an existing 3-D Markov random field simulation to volumetrically model the Lewis Canyon outcrop on the basis of vertical facies transition tendencies. Statistical interrogation of the 3-D model output reveals the simulation to contain realistic facies associations compared to the outcrop. This suggests that the reconstruction process, based on Markov chains, produces a useful representation of 3-D heterogeneity in this Lower Cretaceous carbonate succession. Markov random field simulation might provide an important tool for prediction and simulation of subsurface carbonate reservoirs.**

INTRODUCTION

The complexity of carbonate systems makes detailed direct characterization of their dimensional heterogeneity difficult. Reservoir models strive to fill this knowledge gap by attempting to provide geometrically realistic appraisals of lithologies. The reliability of this approach is, however, linked to the quantity and quality of data used to condition the models. All too often, these data are inconveniently sparse. For instance, drilling provides only discrete data, spatially limited, and totally biased to the vertical direction, such that inferences must be made to predict architecture away from the well. Seismic imaging can provide continuous vertical and horizontal information, but it is limited in its resolution. Against this backdrop, this study considers a class of probability models—a Markov-chain model of transition probability—as a basis for geostatistically populating interwell space. The power of a Markov approach over existing modeling strategies, such as multipoint statistics, stochastic object modeling, and Gaussian or plurigaussian simulation, is that viable simulations can be produced using only sparse training data, such as that delivered by a small number of cores through a reservoir layer. The strategy is also easy to port from 1-D, to 2-D, and onto 3-D (Switzer 1965; Lin and Harbaugh 1984; Politis 1994; Carle et al. 1998; Salomão and Remacre 2001). The underlying premise of Markov simulation for reservoir characterization is the use of facies juxtaposition patterns harvested from vertical sections to elucidate juxtaposition motifs in the horizontal direction (Doveton 1994; Parks et al. 2000; Elfeki and Dekking 2001, 2005; Purkis et al. 2005; Riegl and Purkis 2009).

One explanation as to why a connection may exist between the vertical and lateral changes of facies in outcrop and the subsurface is provided by Walther's Law. As originally stated, the law reads that "*The various deposits of the same facies areas and similarly the sum of the rocks of different facies areas are formed beside each other in space, though in cross-section we see them lying on top of each other. As with biotopes, it is a basic statement of far-reaching significance that only those facies and facies areas can be superimposed primarily which can be observed beside each other at the present time*" (Middleton 1973). It must be noted that application of Walther's Law is valid only for conformable successions of genetically related—homologous—strata. Though two facies may be vertically stacked, it cannot be assumed that they were conformable in time as they now are in space. For example, vertical changes across sequence boundaries potentially reflect major shifts of facies between successions that are genetically unrelated and therefore non-Waltherian. On one hand

Published Online: April 2012

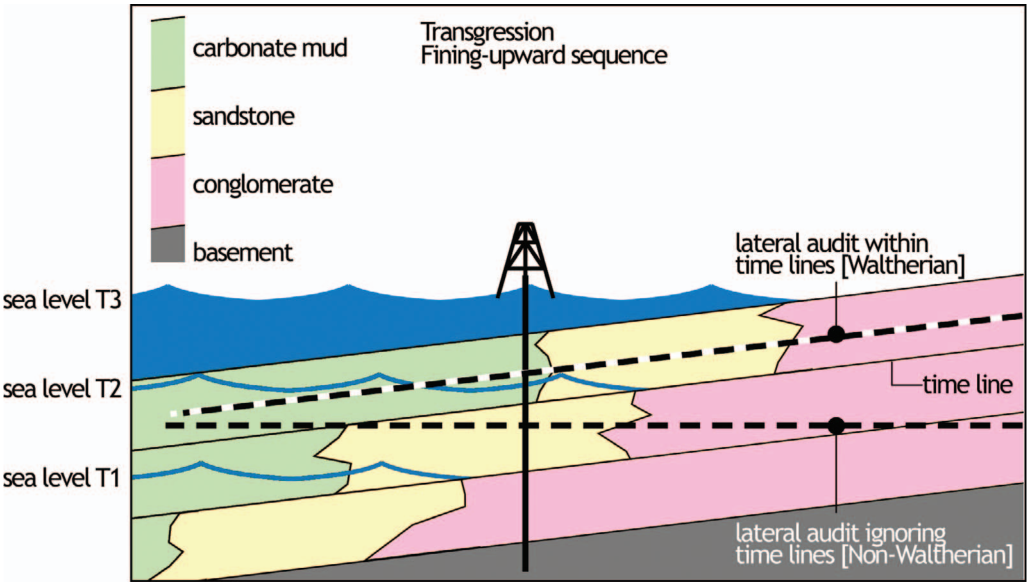

FIG. 1.—Mechanisms of vertical-to-lateral equivalency in facies transitions. This conceptual marine transgressive sequence displays vertical-to-lateral commonality in the arrangement of facies when queried along a time line, such that only genetically related strata are considered (broken black and white line). Interrogated in this way, Walther's Law is honored. The sequence could also be sampled in a non-Waltherian manner, disregarding time lines, which again delivers vertical-to-lateral symmetry of facies transitions (e.g., broken black line), this time due to the seaward inclination of bedding planes.

then, the inevitable presence of depositional discontinuities in the rock record precludes *direct* application of Walther's Law as a means with which to relate vertical and horizontal motifs of facies succession. On the other hand, even systems punctuated with hiatus may still develop *basic vertical-to-lateral relationships* in facies ordering, unrelated to Walther's Law. For instance, under certain circumstances, such as a marine transgressive sequence, facies may vary in an analogous manner both vertically and horizontally, whether or not time lines are considered (Fig. 1). The vertical-to-lateral symmetry observed when time lines are crossed is not Waltherian, considers nonconformable facies, and occurs because basinward-inclined beds are sampled horizontally. In fact, it can be seen that almost any path drawn through the depicted succession, even vertical, crosses the basinward inclined surfaces and the series of lithologies sampled reflects the distal to proximal arrangement of the three facies in the considered figure. Coupled with simple Markov theory, which describes whether stratal units pass from one state to another in a statistically predictable chainlike manner, it can be deduced that under such conditions, comparable facies frequencies and transition probabilities link vertical and lateral facies stacks. If one can be quantified, the other can be estimated. It therefore follows that 2-D or even 3-D Markov-chain models can be developed by assuming that spatial variability in any direction can be characterized by a 1-D Markov-chain. Although this may seem like a tenuous theoretical leap, the assumption here is merely that Markov-chains might characterize spatial variability not only in the vertical, but in other stratigraphic directions such as dip or strike (Carle et al. 1998). This convertibility forms the foundation for the Markov random field simulation (MRFS) considered by this study. Before attempting to condition a geostatistical model in this manner, it is necessary to first verify in a real-world carbonate setting that facies arrangements are Markovian and that vertical-to-lateral equality can be assumed.

The study undertakes three tasks:

(1) We take the Albian stratal architecture exposed in Lewis Canyon (Pecos River, Texas, U.S.A.) to test the degree to which the facies transitions in the vertical and lateral can be considered as Markov-chains.
(2) For the Lewis Canyon outcrop, we statistically determine the degree to which symmetry exists in vertical-to-lateral facies transitions.
(3) To explore the development of a MRFS based upon Carle et al. (1998). This 3-D model is conditioned using outcrop measurements from Lewis Canyon. The objective is to demonstrate Markov-simulation to be capable of yielding geologically plausible results for carbonate facies.

METHODS

Upper Cretaceous of Lewis Canyon

The upper Albian (Cretaceous) rudist reef buildups exposed along the Pecos River Canyon in Texas are both well preserved and well mapped (Rose 1972; Scott 1990; Kerans et al. 1995; Lehmann et al. 2000). Detailed outcrop studies of this exposure, in Lewis Canyon and the wider Comanche shelf, have allowed the development of a tightly constrained stratigraphic framework that can be traced from platform-interior facies, through the intra-shelf-basin margin, and into the intra-shelf basin (Kerans 2002). The total bathymetric range of this ramp intra-shelf basin system ranges from subaerial to approximately 130 m water depth, and facies are bundled into five high-frequency facies successions separated by hiatal surfaces. The rocks in these successions are exposed laterally for several kilometers and vertically for tens of meters. The lowermost of the five successions and the cap of the first succession are composed of a single facies, skeletal grainstone, and are not considered further here. Instead, the following analysis focuses on the four central successions (delineated by horizontal black lines in Fig. 2A, FS-1 through FS-4), all rich in their facies complement and dominated by mud-rich radiolitid–chondrodont mounds that transition from laterally continuous biostromes to laterally isolated small patch-reef elements (red in Fig. 2A). Situated above the maximum-flooding surface, facies succession 1 (FS-1) is genetically different from FS-2 through FS-4. While the rudists in the lower three successions built distinct bioherms, deposits in the uppermost succession comprise less distinct planar biostromal beds and are composed of different species (a dominance by caprinid rudist bivalves as opposed to radiolitid–chondrodont). By far, the best-developed bioherms occur in FS-3.

The outcrop panel was mapped to 11 facies classes (Fig. 2A) but, for our analysis, it was clumped to five facies (Fig. 2B). The clumping serves to vertically thicken and laterally extend the lithologies in the outcrop, a configuration better poised for modeling than a large number of thin and narrow lithologies. Carle et al. (1998) similarly adopted a small number (four) of broad facies in their development of the Markov simulation approach.

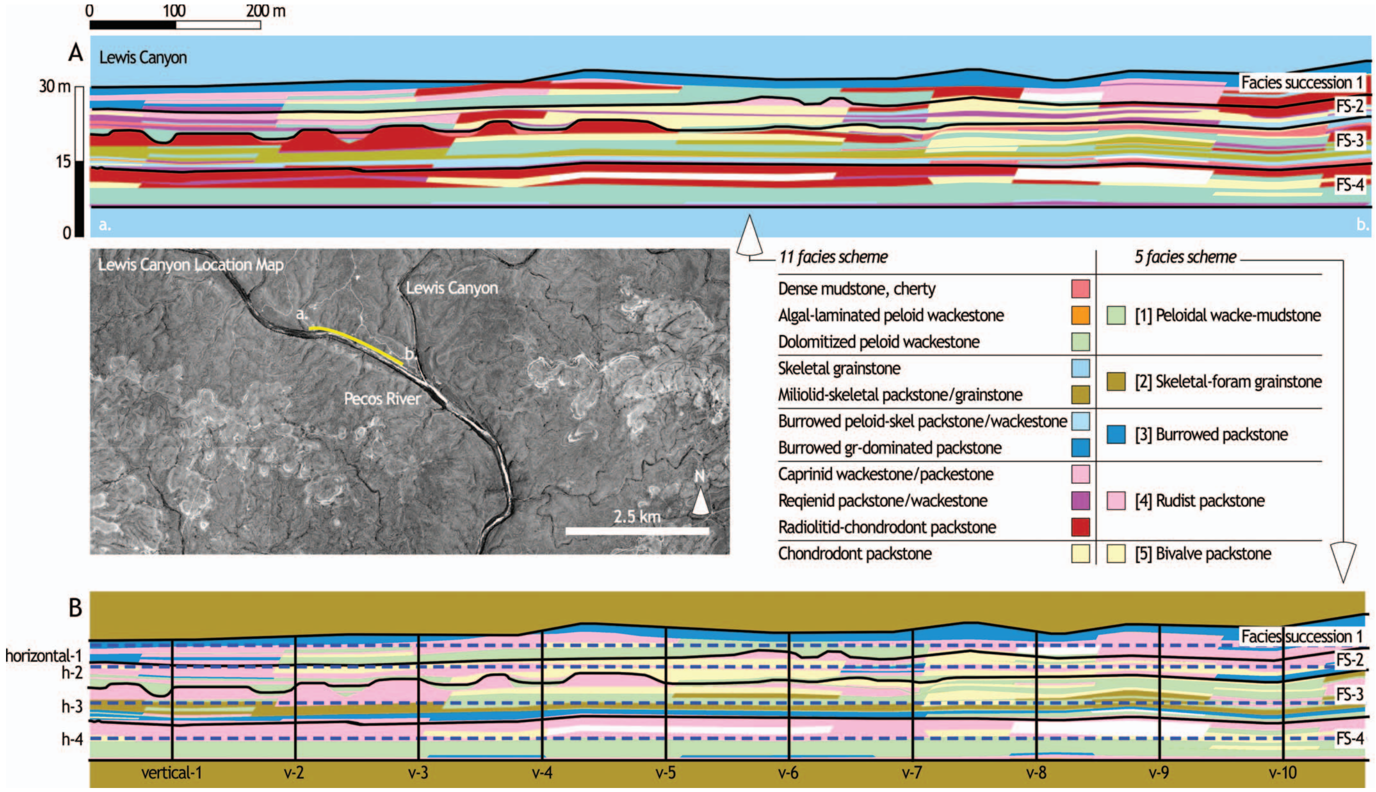

FIG. 2.—**A)** Lewis Canyon Albian outcrop as mapped by Kerans et al. (1995) to 11 facies categories. Horizontal black lines demark facies succession boundaries. **B)** Outcrop remapped to five facies categories and positions of the ten vertical sections (vertical black lines) and horizontal bed-parallel transects (broken blue lines) along which facies juxtapositions were tabulated. Inset is a gray-scale satellite image showing the location of the mapped section (yellow line) adjacent to the Pecos River.

Treatment of Succession Boundaries

Facies succession boundaries in the considered outcrop track hiatuses. Both for the statistical treatment of facies ordering and for subsequent Markov simulation, we stratify our analysis, treating each succession separately. Our vertical sections are therefore partitioned between the four facies successions (Fig. 3A), as are the lateral transects (Fig. 3B). This is consistent with the typical approach for the modeling of carbonate rocks, where the accurate positioning of succession boundaries is perhaps as important as the bundling of facies between them. We consider statistics derived from ten vertical sections, evenly distributed across the outcrop panel (positions shown in Fig. 2B, sections in Fig. 3A). These sections are considered as analogous to cores through a reservoir layer. To laterally sample the outcrop, transects are installed horizontally across the nearly tabular bedding planes (positions in Fig. 2B, sections in Fig. 3B).

The Markov Property of Successions

As applied in this study, Markov-chain analysis is used to detect repetitive arrangements of facies in space. As per Rankey (2002), this is accomplished by characterizing the complexity of transition probabilities between subfacies and testing whether they are nonrandom. Detailed treatments of Markov processes can be found in Kemeny and Snell (1960), Roberts (1976), and Iosifescu (1980). Examples of Markovian statistics applied to vertical variability in sedimentology have been used for many decades (Krumbein and Dacey 1969; Doveton 1971; Powers and Easterling 1982; Wilkinson et al. 1997; Lehrmann and Rankey 1999; Purkis et al. 2005; Bosence et al. 2009), but there has been relatively little use of Markov-chains for lateral prediction and stochastic simulation (Carle et al. 1998; Riegl and Purkis 2009).

If a succession is proven to be nonrandom in terms of its facies transitions, it possibly holds the "Markov Property"—the implication of this being that the probability of appearance of a particular facies category in the succession can be computed from previous occurrences. Stratigraphic successions that display the Markov property hence adhere to well-defined rules of facies transition probability. The latter point is relevant in light of the fact that many geometric aspects of modern carbonate depositional environments have been reported as strongly deterministic (Rankey 2002; Purkis et al. 2005; Purkis et al. 2007; Purkis et al. 2010; Purkis and Kohler 2008; Harris and Vlaswinkel 2008; Fullmer et al. 2010; Harris et al. 2010, 2011).

The existence of Markovian ordering in a sequence is tested through statistical analysis of transition frequency matrices (TFMs). These tally the prevalence of juxtapositions between facies categories, such as a measured section or horizontal traverse across an outcrop panel (Fig. 3). The tendency of one state (facies) to succeed another in the section can be emphasized in the TFM by converting the frequencies to percentages. By doing so, a relative transition matrix (RTM) is created, the sum of which will be 100%. The RTM is calculated by dividing the raw counts of the TFM by the grand total of the TFM matrix.

There is one further method called upon in this study used to depict transitions in matrix form. This is the transition probability matrix (TPM). Whereas the TFMs report on the overall number of transitions between states, the TPM expresses the probability of facies juxtaposition, irrespective of the prevalence of the classes in the measured section. The TPM is constructed by dividing each row of the TFM by the row total, thereby normalizing the row to sum to one. There are two ways to test for the Markov property in lithologic successions. Firstly, via point counting at regular intervals, "normal" Markov statistics can be harvested. If the sampling interval is sufficiently fine, this method yields viable information on the thickness of each facies, in addition to their neighborhood

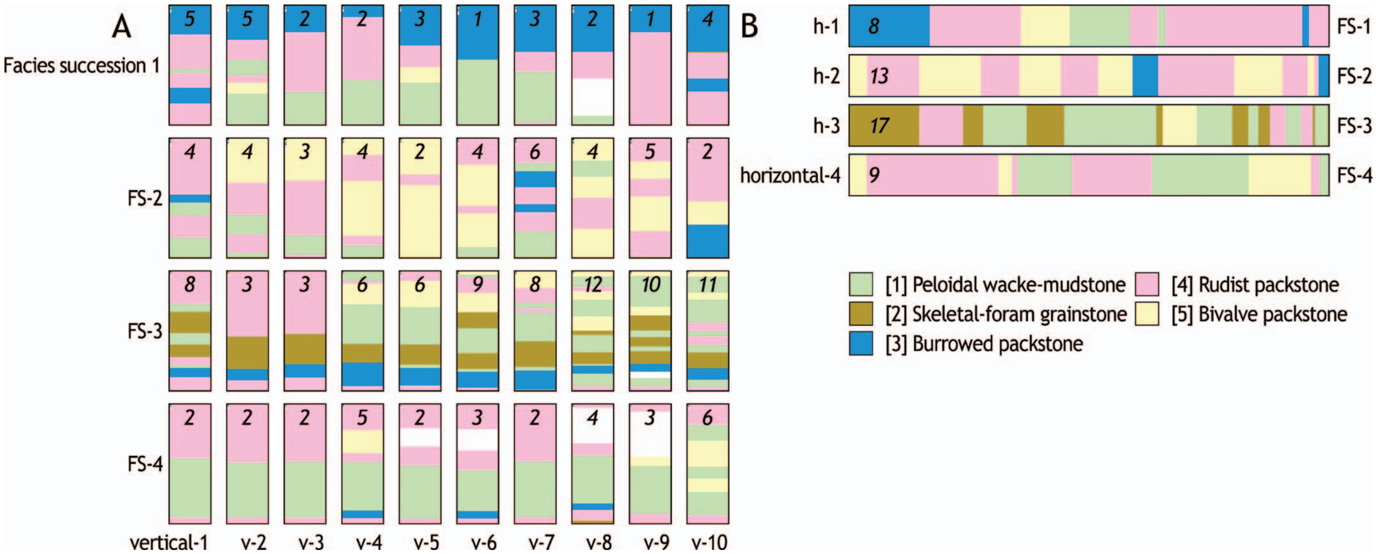

FIG. 3.—**A)** Facies stacks for ten vertical sections evenly distributed across the outcrop panel occurring between succession boundaries (vertical black lines in Fig. 2B). **B)** Horizontal transects, one per succession (broken blue lines in Fig. 2B). The number of facies transitions in each profile is italicized. The vertical and lateral scales of the transects are relative, stretching for several meters between facies successions boundaries for the vertical sections and ~ 1.5 km for the lateral. See Figure 2 for true scale.

properties. By comparison, embedded sampling (Krumbein and Dacey 1969; Davis 2002) discards all information about the thickness of a sequence, tallying only juxtapositions that occur between *different* lithologies. This action has the disadvantage of curtailing information content of the stratigraphic audit, particularly when the thickness of each interval bears process information. This study favors normal Markov statistics for both the interrogation of the outcrop and implementation of a Markov random field simulation.

To test for the normal Markov property, a comparison is made between the "observed" TPM (i.e., that calculated from the queried section) and an "expected" TPM which is populated with the transitions which would be delivered if the occurrence of a lithologic state at one point in the stratigraphic interval were completely independent of the lithology at the immediately underlying point (Davis 2002). The comparison between observed and expected TPMs tests the hypothesis that all lithologic states are independent of the preceding states. This is achieved using a X^2 test. For the given degrees of freedom (taken to be $(m - 1)^2$, where m is the number of states in the measured section, five in Fig. 3) and significance level (throughout this study set to the 99.9% level), if the test statistic exceeds the critical value of X^2, it can be concluded that there is a statistically significant tendency for certain lithologic states to be preferentially followed by certain other states—the queried section is a Markov-chain. If, however, the test statistic fails to exceed the critical value of X^2, the hypothesis is upheld that all states are independent of the preceding states and it is concluded that the section lacks predictability in its succession of lithologies.

Nonrandom Stratal Ordering in Lewis Canyon?

Following the workflow of Davis (2002), the 40 vertical sections (ten per facies succession, four successions) and four lateral transects (one each for four successions) obtained from the Lewis Canyon outcrop were tested as normal Markov-chains using X^2. With reference to the detail in which the outcrop was originally logged, the vertical sections were sampled at 10 cm while the much more extensive lateral transects were sampled at 1 m. Integers were used to encode one of five facies categories for each pixel (colored in Fig. 3). Succession statistics were tabulated by iteratively walking out each transect and tallying facies associations between each pixel.

The null hypothesis that the observed transitions for the combined vertical sections, as well as the bed-parallel lateral transects, are distributed randomly can be rejected for all four successions at the 99.9% significance level. Confirmation of Markovian order in the sections is logical and to be expected. In the context of determining Markovian dependence within a stratigraphic sequence, virtually no real-world exposure of any significant length consists of randomly ordered lithologies. At almost any scale of consideration longer than several dozen stratal elements (here we consider many more), sequences exhibit up-section change, in either the dominance or the thickness of one or more particular rock types. This, combined with the great number of self-to-self facies transitions, all but ensures the presence of the Markov property when considered using normal statistics.

Statistical Comparison of Frequency Matrices

The vertical and lateral transects of the Lewis Canyon outcrop are of significantly different extents. Bounded by the divisions of the four facies successions, the ten vertical sections are of only ~ 6 m meters in height, while the four bed-parallel transects each extend for ~ 1,500 m (Fig. 2). Given the 10 cm sampling interval to which the vertical audits were queried, each 6 m vertical section in a single succession yields ~ 60 observations of facies character. The 1 m sample interval for the 1,500-m-long lateral transects conversely delivers 1,500 observations. Per succession, less information is therefore harvested in the vertical direction than in the horizontal. Even though the mapped resolution of the outcrop is considerably greater in the vertical than the horizontal, the disparity between the two orientations cannot be closed by simply auditing the vertical at a finer sampling interval. Furthermore, and as is visually apparent (Fig. 3A), the majority of the ~ 60 state transitions from any given vertical section will be between two sampling intervals of the same facies category, so called "self-to-self" transitions.

To raise the statistical power of the treatment of the vertical audits of the outcrop, we follow Verwer et al. (2009) and create a "global" tally of juxtaposition occurrences. This was accomplished for each of the four facies successions by summing over the vertical TFMs of the ten sections; essentially treating the ten as a single, more extensive, section with which to characterize the succession (the number of observations therefore increased ten-fold from 60 to 600). This was done for three reasons. First, and as per Davis (2002), this treatment ensures that each facies category in the vertical dataset has an expected frequency of at least five transitions. Second, the action delivers a representative vertical audit of each succession to accompany the lateral assessment. The issue of striving for a representative inventory is an important one; while a lateral transect interrogates the full extent of each facies succession and hence will likely capture its heterogeneity, single vertical sections penetrate just a fraction of the succession. Only in the case of perfectly tabular bedding planes can a single vertical assessment be considered a representative summary of stratal ordering throughout the exposure. Third, the goal of the vertical-to-lateral comparison is to ascertain if the MRFS strategy is appropriate, and it is envisaged that the simulation would be conditioned from multiple cores in order to ensure representative sampling of the deposit of interest. By summing over the TFMs, the same transition motif (e.g., packstone succeeding wackestone) will be sampled multiple times if it arises in numerous vertical sections. It would similarly be considered several times if the transition reoccurs in a single section. This study uses two ways of ascertaining whether the transitions within two frequency matrices are statistically different. The first, 2-D cross-correlation, yields a single statistic that summarizes the "global" similarity (i.e., all facies simultaneously considered) between matrices. The second technique, development of continuous-lag Markov-chain models, assesses the similarity of juxtapositions on a facies-by-facies basis, itself yielding an assessment of correlation quality. We employ both techniques to ascertain the degree to which vertical sections from the Lewis Canyon outcrop are equivalent in their statistics of succession to horizontal transects. Both tests are applied to each of the four considered facies successions.

2-D Cross-Correlation and Monte Carlo Simulation

Once a corridor of transitions has been extracted from a logged section, a TFM can be created by "walking" the length of the corridor and tallying facies transitions. The RTM of the corridor is calculated from the TFM as previously described. Provided that the same facies categories (states) are present, to compare the similarity of facies transitions from two different samples, a cross-correlation statistic (r) can be calculated for paired RTMs via [Equation 1]:

$$r = \frac{\sum_m \sum_n (A_{mn} - \overline{A})(B_{mn} - \overline{B})}{(\sum_m \sum_n (A_{mn} - \overline{A})^2)(\sum_m \sum_n (B_{mn} - \overline{B})^2)} \qquad (1)$$

where A and B are paired RTMs with means $\overline{A}$ and $\overline{B}$.

Two RTMs with identical probabilities of transition will return $r = 1$, whereas highly dissimilar RTM pairs will return r approaching 0. This comparison is global and the performance of the correlation is assessed for all facies in the RTM simultaneously.

Though 2-D cross-correlation (Equation 1) returns an r statistic that assesses similarity between two tallies of observed transition probabilities, it does not provide insight into whether an observed difference is statistically significant. Following Gotelli and Ellison (2004), one way to tackle this shortfall is through the use of Monte Carlo simulation (MCS). We employ this technique to generate a randomized dataset of 10^5 paired RTMs that represent the magnitude of r expected due to chance (i.e., if two RTMs shared no common transitions). The procedure generates an RTM with each matrix position populated by a random number. The sum of the RTM is constrained to equal 1 and, as for an actual dataset, the RTM is symmetric across the major diagonal. For the resulting population of r, derived from $n = 10^5$, the 68%, 95%, and 99.7% confidence intervals (CI) are taken as 1, 2, and 3 standard deviations respectively of the right-hand tail (Fig. 4).

Results of 2-D Cross-correlation and MCS

2-D cross-correlation of the vertical-to-lateral RTMs reveals a statistical level of equivalency across the four Lewis Canyon successions (Fig. 4). In all cases, values of r fall beyond the 95% CI of the randomized "estimate" MCS population.

These results demonstrate that the similarity in facies transitions between the vertical and lateral sections of Lewis Canyon is significantly greater than would be expected from the comparison of sequences composed of randomly ordered facies. At the 95% confidence interval, Markov transitions in the vertical and lateral are statistically inseparable, and the outcrop can therefore be correctly represented as a multidimensional (i.e., vertical–lateral) Markov-chain. Furthermore, vertical-to-lateral equivalency is observed in each of the four successions considered, despite their different stratigraphic frameworks and facies types. For instance, the uppermost succession is characterized by a shingled low-accommodation rudist packstone assemblage (FS-1, Fig. 2). Meanwhile, the lowermost succession (FS-4), is dominated by peloidal wacke-mudstone. In both, the pattern of lithologic succession in vertical and lateral directions is nonrandom and statistically equivalent ($p = 0.05$).

Markov-Chain Models

The weakness of the global comparison of paired RTMs (Equation 1) is that a poor correlation of a single facies class serves to penalize the overall agreement that may exist between two, otherwise comparable, transition matrices. The technique also fails to examine how facies-specific relationships interact within a sampled transition matrix. To allow a facies-specific calculation, the TFMs from the two orientations to be compared (vertical vs. lateral) must be row-normalized to TPMs (procedure previously described). Next, from the TPMs, continuous-lag Markov-chain models are developed via transiograms—transition probability diagrams—according to Carle et al. (1998) for every permutation of facies transition. Transiograms are a means of defining a transition probability function over a spatial distance (lag) and serve to fulfill the same role in Markov-chain geostatistics as an indicator variogram in kriging geostatistics. In a context of MRFS, the transiogram provides a flexible means of estimating transition probabilities with continuous lags from samples, which are needed by Markov-chain conditional-simulation models (Carle et al. 1998; Weissmann and Fogg 1999; Li and Zhang 2007). They capture and visually portray both the autodependence of different lithofacies in a sequence across space and the interdependence between them.

Transiograms are calculated by iteratively powering the TPM, thus obtaining the modeled transition probabilities at distance multiples of the original lag h_{sample} at which the TFM was computed (i.e., the sampling interval). The transiograms are obtained following the Chapman-Kolmogorov equation applied to Markov chains (Papoulis 1984), as

$$T_n = T_{(n-1)} \cdot T, \quad n > 0 \qquad (2)$$

where T is the $k \times k$ matrix of transition probabilities (TPM) for the k lithofacies, and T_0 is the $k \times k$ identity.

This equation is the basis for the discrete-lag formulation of the Markov-chain model (Carle et al. 1998). For the simulations presented in this paper we have used a continuous-lag model, which presents the advantage of allowing the computation of the transition probabilities at any lag interval. The continuous-lag model is expressed as:

$$T(h) = \exp(R \cdot h) \qquad (3)$$

where R is the $k \times k$ matrix of transition rates (Carle et al. 1998) and h is the lag at which the continuously valued $T(h)$ is evaluated. Noting

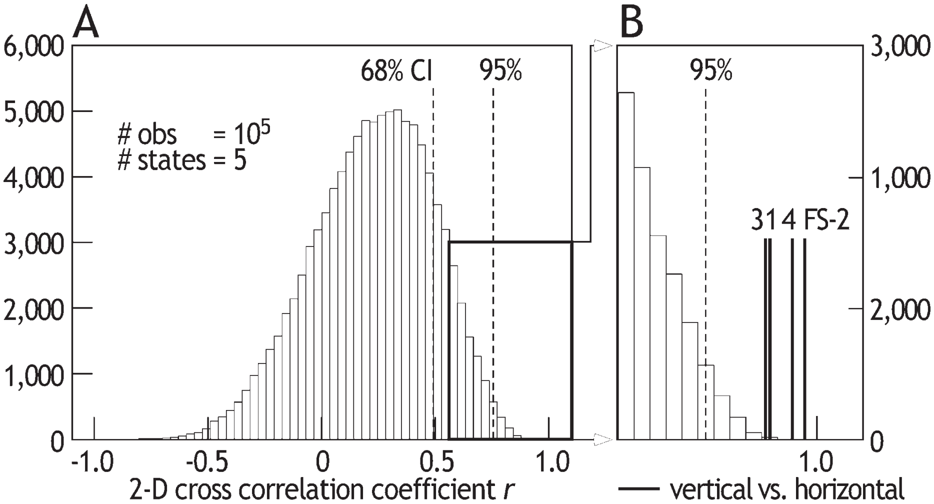

C

Permutation	r	
FS-1 vertical vs. horizontal	0.90	95% CI = 0.76
FS-2 vertical vs. horizontal	0.97	
FS-3 vertical vs. horizontal	0.89	
FS-4 vertical vs. horizontal	0.95	

FIG. 4.—**A)** Histogram of the Monte Carlo Simulation (MCS) population of 2-D cross-correlation coefficients (r) produced by 10^5 pairings of randomized RTMs [Equation 1]. Broken vertical lines depict 68% and 95% confidence intervals. **B)** Magnifies the right-hand tail of the MCS distribution, and plots r values for the four facies successions (FS) obtained by cross-correlating RTMs from vertical sections and horizontal transects (black lines). **C)** All results are significant at the 95% confidence interval.

that $T = T(h_{sample})$, the matrix of transition rates is computed from the TPM as

$$R = \frac{\ln(T)}{h_{sample}} \tag{4}$$

The transiogram concept is demonstrated using "h-3," a horizontal audit of succession 3 of Lewis Canyon (Fig. 5). This four-facies-category example generates a matrix of 16 transiograms. The major diagonal position in the matrix describes the autotransition probability of different lithofacies in the stratal sequence with the form of the Markov-chain model reflecting the thickness and prevalence of each category. As with Carle et al. (1998), the mean length of each category in the transect is indicated on the plot of autotransition probability vs. lag by the intersection of the tangent at the origin with the ordinate axis (dashed lines in the diagonal entries of Fig. 5). Since the mean length of peloidal wacke-mudstone is greater than that of rudist packstone, for example, the gradient of the dashed line is shallower and intersects the ordinate axis farther from the origin. The estimated mean length yielded by point of intersection can be seen to correspond well to that measured (Table 1). Off-diagonal elements in the matrix describe crosstransitional probabilities between the four lithofacies. The plotted curves represent the transition probability from one category to another at specified lag distances. For example, there is a higher likelihood of association between peloidal wacke-mudstone with skeletal–foram grainstone at small lag distances, than between peloidal wacke-mudstone and bivalve packstone, a property that becomes obvious when the transect is visually inspected.

The use of the transiogram to compare lithofacies associations in two separate datasets can be demonstrated by creating Markov-chain models for a pair of categories from the Lewis Canyon outcrop (Fig. 6). To establish the workflow, we compare crosstransitional probabilities for the lateral ordering of facies succession 3 peloidal wacke-mudstone and skeletal–foram grainstone. The first dataset is transect h-3, which is horizontally oriented through the third succession. This is compared to transect bp-3, laterally oriented also, but parallel to the undulating bedding planes of the succession (Fig. 6A). As is evident by visually comparing h-3 and bp-3, the pattern of occurrence for the two considered fabrics is different (Fig. 6B). Most notably, the skeletal–foram grainstone is more prevalent in h-3 than in bp-3. The transects are unalike because of their differential passage through the outcrop. The trends of the Markov-chain models diverge also (Fig. 6C).

The error metric used to appraise the accordance between the two Markov models developed within the transiogram is the *mean absolute difference* (*MADiff*):

$$MADiff_{ij} = \frac{\sum_{n=1}^{L} |T_{vert}(n,i,j) - T_{lat}(n,i,j)|}{L} \tag{5}$$

where, $T_{vert}(n, i, j)$ and $T_{lat}(n, i, j)$ refer to the probability of changing from facies i to facies j at lag n, as described by the 1-D discrete-lag Markov-chain models developed for the vertical and lateral directions. The value L is the maximum lag considered for comparing the models within the transiogram. Since T_{vert} and T_{lat} refer to probability values, the *mean absolute difference* is naturally limited to the interval [0 1]. A value of $MADiff_{ij}$ = 0 describes a perfect fit, and $MADiff_{ij}$ = 1 the worst possible fit, between the two Markov models within the lag interval [1 L].

Facies-Specific Comparison of Markov-chain Models

While 2-D cross-correlation with MCS provided a "global" appraisal of vertical-to-lateral equivalence for the Lewis Canyon outcrop (Fig. 4), transiograms and Markov-chain models provide information on individual facies pairs. For the five facies categories there are 25 possible permutations of facies pairings, each yielding a value of *MADiff* and tallied in a matrix, one for each of the four successions. These values are calculated via Equation 5 and assess the accordance of 1-D discrete-lag Markov-chain models developed over 50 lags in the lateral and vertical directions. Because of the resolution at which the outcrop was digitized, in the lateral 1 lag = 1 m, while 1 lag = 10 cm in the vertical. For each succession, the facies-by-facies performance was assessed for vertical sections vs. horizontal transects (Fig. 7). The results are presented as gray-scale coded matrices by facies

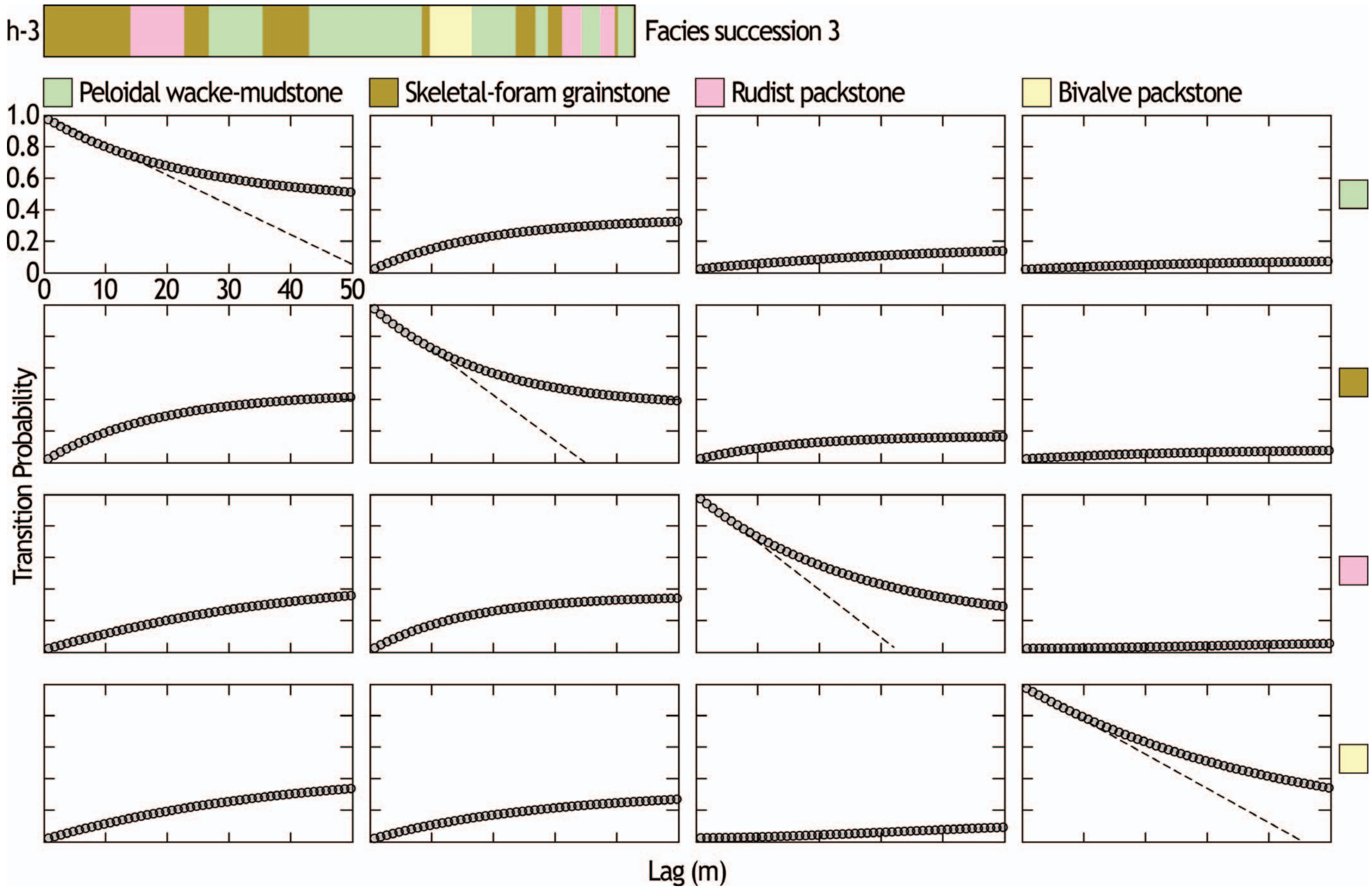

FIG. 5.—Matrix of transiograms for a horizontal transect through facies succession 3 of the Lewis Canyon outcrop (i.e., h-3, Fig. 3B): measurements (black circles) and Markov-chain models (gray lines).

succession, with light shades indicating better agreement between the Markov-chain models developed in the vertical and lateral direction of the outcrop than dark shades, which denote poorer accordance.

The *MADiff* index is absolute, not relative. For a given succession and over all lag distances, if a given facies pairing is rare in both the vertical sections and lateral transect, the value of *MADiff*, because it measures absolute difference, is also constrained to be low. Though not captured by the index, the *relative* difference between transiograms for that pairing may be great. We consider the absolute comparison logical since the most important criteria for vertical-to-lateral equivalency for the facies pairing is that it is rare in both orientations. Relative differences in scarcely observed pairings are of secondary importance only, and we do not consider it useful to give prevalent and rare facies equal weight in the analysis.

The matrices of *MADiff* values show that not all facies pairings are similar (Fig. 7). The greatest divergence between the vertical and lateral can be seen down the major diagonal of the matrices, the position describing self-to-self transitions—the autodependence of different lithofacies in the sequence. By contrast, off-diagonal elements describe vertical-to-lateral interdependence between lithofacies—transitions from one category to a different category. Large divergence (high *MADiff* values) down the major diagonal should hence be expected if there are pronounced differences in bedding thickness when assessed in the vertical vs. the lateral, as indeed is the case for the considered outcrop. First, the panel is much more extensive in the lateral than in the vertical direction, and second, because the sampling frequency differs in the two directions. These differences will not confound the volumetric MRFS model (to be discussed shortly) because by-facies differences in vertical-to-lateral extent can be conditioned.

Comparing vertical sections vs. horizontal transects (Fig. 7), all successions perform approximately equally with typical *MADiff* values in the range of 0.10 to 0.20 (a 10–20% level of discordance). Facies codes 4 and 5 (rudist and bivalve packstones, respectively) display the highest (i.e., poorest) values of *MADiff*, but still rarely exceeding 0.30. These are the most prevalent facies in both the vertical sections and horizontal transects and hence have the greatest chance of transition to not only each other, but also all other facies in the succession. Across all successions, cases exist where a particular facies is not present in one or both of the compared vertical and lateral transition matrices. Here, since two Markov models cannot be generated for the facies pairing, the corresponding positions in the matrix are marked as "transition absent" (TA, Fig. 7).

DISCUSSION

Markov Facies Ordering and Vertical-to-Lateral Equivalency

Through confirmation of the normal Markov property for each of the four considered successions, the study has shown that the stratal stacking of the Lewis Canyon outcrop to exhibit nonrandom up-section transitions from one rock type to another. The Markov property exists also in the ordering of facies in the lateral direction. The implication of the finding that the outcrop includes ordered facies stacking is that it can be considered and modeled using Markov-chains. From the perspective of MRFS, the Markov property becomes useful, however, only if it is transferrable between the vertical and lateral directions. Two separate

TABLE 1.—*Mean lengths by facies succession (FS) for the specified (vertical) and simulated (lateral) directions used as input to the 3-D MRFS model. Facies prevalence for each simulated succession is harvested from the vertical outcrop sections.*

Facies succession	Broad facies category	Mean extent vertical	Mean extent dip	Mean extent strike	Prevalence vertical
FS-1	[1] Peloidal wacke–mudstone	1.87 m	58.33 m	58.33 m	28%
	[2] Skeletal–foram grainstone	0.00 m	0.00 m	0.00 m	0%
	[3] Burrowed packstone	1.63 m	71.00 m	71.00 m	33%
	[4] Rudist packstone	1.64 m	114.83 m	114.83 m	37%
	[5] Bivalve packstone	0.66 m	84.67 m	84.67 m	2%
FS-2	[1] Peloidal wacke–mudstone	0.70 m	0.00 m	0.00 m	13%
	[2] Skeletal–foram grainstone	0.00 m	0.00 m	0.00 m	0%
	[3] Burrowed packstone	0.81 m	25.33 m	25.33 m	5%
	[4] Rudist packstone	1.36 m	67.33 m	67.33 m	41%
	[5] Bivalve packstone	1.75 m	58.00 m	58.00 m	41%
FS-3	[1] Peloidal wacke–mudstone	0.66 m	59.78 m	59.78 m	30%
	[2] Skeletal–foram grainstone	0.87 m	39.14 m	39.14 m	22%
	[3] Burrowed packstone	0.69 m	0.00 m	0.00 m	11%
	[4] Rudist packstone	0.85 m	41.11 m	41.11 m	26%
	[5] Bivalve packstone	0.58 m	58.67 m	58.67 m	12%
FS-4	[1] Peloidal wacke–mudstone	2.14 m	89.11 m	89.11 m	43%
	[2] Skeletal–foram grainstone	0.16 m	0.00 m	0.00 m	0%
	[3] Burrowed packstone	0.35 m	0.00 m	0.00 m	2%
	[4] Rudist packstone	2.27 m	97.33 m	97.33 m	49%
	[5] Bivalve packstone	0.90 m	52.00 m	52.00 m	6%

statistical tests returned the same verdict for the outcrop; though differences exist, the facies transition probabilities in the vertical and lateral directions are statistically equivalent ($p < 0.05$). Since the stacking of stratal elements was also shown to be Markovian, the lateral ordering of facies in Lewis Canyon, if unknown, could be correctly reconstructed from vertical information alone.

The transferability of vertical-to-lateral facies transition probabilities is extended to query the performance of individual facies pairs (Fig. 7). Although prevalence is not stable for all facies between the lateral and vertical directions for the four successions, the overall accordance remains high. Disregarding for now the self-to-self transitions that inhabit the major diagonal of Fig. 7, the mean absolute difference between vertical and lateral models for all successions is < 0.40 (i.e., 40%) and in the majority of cases < 0.20. On a facies-by-facies basis, juxtaposition motifs in this Albian outcrop harvested from the vertical are in good accordance with those observed in the lateral. Values of *MADiff* down the major diagonal of the figure are higher and indicate a greater level of discordance between vertical and lateral Markov models. This is to be expected, because the major diagonal of the *MADiff* matrices report on the self-to-self facies transitions and will naturally diverge in the expected case of differences in bedding thickness between the vertical and lateral direction of the outcrop.

3-D Markov Random Field Simulation

To this point we have observed the stratal stacking and lateral ordering of the Lewis Canyon outcrop to exhibit non-random (Markovian) facies transitions and the motifs of juxtaposition to be statistically similar in the vertical and lateral plane. Both observations hold for each of the four considered facies successions. The implication is that geostatistical techniques of reservoir reconstruction based on Markov-chains might offer very realistic characterization of lateral heterogeneities for the outcrop. To explore this premise, our paper finishes with a proof-of-concept investigation into 3-D Markov random field simulation (MRFS) to solve for lateral variability in facies, given observations from the vertical. The simulation will be stratified by succession and conditioned using statistics harvested from the ten vertical sections through the outcrop (v-1 through v-10, Fig. 3). The resultant stochastic MRFS approach is built around the workflow of Carle et al. (1998) and is implemented using computer code written in MATLAB. The model relies on the development of 3-D Markov-chains that enable creation of a multi-category simulation of spatial variability within a volume, while incorporating directional-dependencies (anisotropy) as well as juxtapositional relationships.

For each facies succession, the model is developed in five steps from juxtaposition likelihoods harvested in the vertical direction: (1) calculation of 1-D discrete-lag Markov-chains using transiograms for the vertical facies transitions, (2) development of transiograms for the unconditioned lateral-dip and lateral-strike directions with reference to user-supplied mean length values for each facies (harvested from the outcrop), (3) calculation of 2-D continuous-lag Markov models encompassing the vertical and lateral directions, (4) sequential indicator simulation, which serves as an initial configuration for (5), simulated quenching (zero-temperature annealing). Whereas this approach has been used in a few clastic settings for the simulation of hydro-facies (Carle and Fogg 1997; Carle et al. 1998; Weissmann et al. 1999; Weissmann and Fogg 1999), to our knowledge it has not been applied to carbonate rocks.

The MRFS model for each succession demands, as input, a mean extent of each facies category in the vertical, dip, and strike directions (Carle et al. 1998). Those for the vertical, the "specified" direction, are extracted from the same facies stack as used to supply the juxtaposition rules against which the model is conditioned (i.e., Fig. 3A). Mean extents for the "simulated" lateral directions are harvested from the horizontal transects previously used to query the outcrop (Fig. 3B). The values are supplied in units of meters and condition the persistence of each facies in the model for both the specified and the simulated directions (Table 1). When applied in the subsurface, values of lateral persistence are likely unknown and must be populated with reference to an analog. With lack of any geological evidence to the contrary, the mean extents for the dip and strike directions in the model were set to be equal. The simulation of each succession therefore will be isotropic in the lateral direction but anisotropic in the vertical, because both are characterized by different facies extents. It should be noted, however, that the MRFS can handle lateral anisotropy. The prevalence of each facies in the four simulated

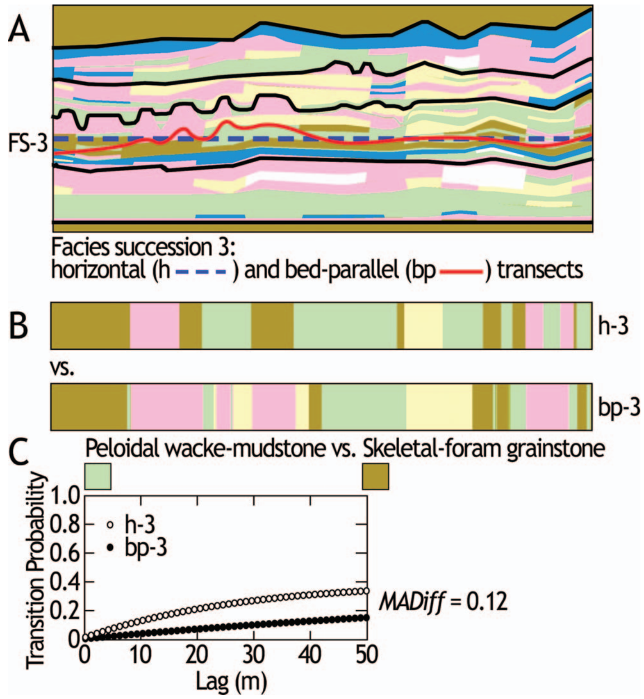

FIG. 6.—Example of a transiogram developed for juxtaposition tendencies for two facies, peloidal wacke-mudstone and skeletal–foram grainstone, as audited using different methods from facies succession 3 of the outcrop (horizontal, h, vs. bed-parallel, bp). White circles are derived from a TPM summarizing facies associations from the horizontal transect, black circles from the bed-parallel one. The mean absolute difference (*MADiff*) for the two Markov-chain models is 0.12.

succession is set equal to the mean proportions harvested from the ten vertical sections through the outcrop (Table 1).

For each of the four successions, the MRFS model was run on a 3-D grid with side lengths of 273 "voxels" for the dip and strike directions, and 91 voxels in the vertical. Each of the four generated simulation "cubes" were hence composed of a total of 6,782,139 voxels, with each voxel assigned one of the five facies categories listed in Table 1 by the MRFS algorithm. The side dimensions of each voxel is 5.49 m in the two lateral directions and 0.07 m in the vertical. A single voxel thus has an area of 1.99 m^3 and each of the four simulated successions encompass a volume of 13,500,000 m^3 (6 m vertical $\times$ 1,500 m dip $\times$ 1,500 m strike). To simulate the entire outcrop in a single volume, the four simulated successions would be stacked one atop the other. This strategy honors the principle of abrupt facies offsets between successions, each modeled independently of the strata in the preceding and following succession. As conditioned by the outcrop observations, the four simulations are strongly anisotropic, with the geobody extents more persistent in the lateral than vertical (Fig. 8).

It is encouraging that despite being conditioned using only vertical facies transition probabilities and mean vertical and lateral extents, the simulations visually capture the first-order geometries of the four successions. As for the outcrop, the FS-1 simulated volume is composed of tabular beds of peloidal wacke-mudstone (green in Fig. 8) that pass to rudist packstone (pink) towards the upper portion of the section. The succession is topped in both the outcrop and simulation by a thin but laterally extensive cap of burrowed packstone (blue). Realistic facies associations and dimensions of rudist and bivalve packstone bodies (pink and yellow) are also delivered in the FS-2 simulation. In FS-3, the only succession in the outcrop in which distinctly mounded rudist packstone (pink) bioherms have developed, the simulation indeed delivers discrete mounded rudist patches of several meters relief. Visually at least, this is a faithful representation of the different motif of deposition which characterizes this succession. Lastly, both for the outcrop and the simulation, FS-4 shows the same tabular motif of laterally extensive sheets of peloidal wacke-mudstone overlain by similarly dimensioned rudist packstone deposits. The simulation of this facies succession also correctly delivers interwoven and laterally discontinuous beds of bivalve packstone.

As for the assessment of lateral-to-vertical commonality conducted for the outcrop, quantitative validation of the MRFS model is achieved through the comparison of paired transiograms. These are developed for each facies category within each of the four facies successions using the *MADiff* error metric (Equation 5). As before, the results of this comparison are presented using gray-scale matrices, light shades indicating better agreement between the specified-input and simulated-output data than dark shades, which denote poorer accordance (Fig. 9). Validation in the vertical direction was accomplished for each succession through comparison of transiograms developed from the ten vertical sections imposed on the Lewis Canyon outcrop panel (Fig. 3A), versus transiograms produced from 20 randomly placed vertical "cores" through the four simulated volumes. Validation of the performance of the model for the four successions in the lateral direction was accomplished by comparing transiograms developed from the horizontal transects logged from the outcrop (Fig. 3B) with 20 randomly placed lateral transects through the simulated volumes (per succession, ten each in the dip and strike directions).

Validation of the MRFS output for the four successions shows variable accordance of facies juxtaposition likelihoods between specified sections and simulated volumes. Greatest divergence is seen for the diagonal positions of the matrices that report on the autotransition probability within a single facies category. In the vertical direction, for bivalve packstone (category 5), *MADiff* twice exceeds 0.40 (successions 1 and 3, Fig. 9A). The disparity arises because this facies is rare in the specified direction and hence uncommon also in the simulated volume for these successions. Off-diagonal elements in the matrix describe crosstransitional probabilities between the specified and simulated lithofacies and are in better accordance. Typically $MADiff < 0.20$, meaning that the maximum mean absolute difference between the specified and the simulated transiograms over the 50 lags is 20%. Positions in the matrices flagged with "TA" denote facies absent from the conditioning data and hence absent too in the simulation. Validation of the lateral direction is similarly bounded by a maximum level of discordance of 20% for crosstransitional probabilities. Note that the only connection between the lateral outcrop sections and the simulation are the mean length values input to the model. Facies transitions in the simulation for the dip and strike are abstractions of the vertical TPM, constructed with reference to the lateral mean length values (Table 1). As with Carle et al. (1998), this validation shows MRFS to be capable of extrapolating facies-transition rules harvested in 1-D (a core), into a 3-D volume, while honoring conditioned motifs of juxtaposition.

CONCLUSIONS

This paper first investigates whether the Albian stratal architecture exposed in Lewis Canyon exhibits nonrandom up-section transitions from one rock type to another. Markovian dependence within the considered stratigraphic sequences was determined, evidencing the successions to be nonrandom. The same result was returned for the lateral ordering of facies in the outcrop. Second, the work tests whether lithofacies transition probabilities in the outcrop were interchangeable between the vertical and lateral direction. Two statistical means of assessment were levied: 2-D cross-correlation with Monte Carlo simulation and a facies-specific comparison using Markov-chain models. Both proved vertical-to-lateral equality of transition probabilities

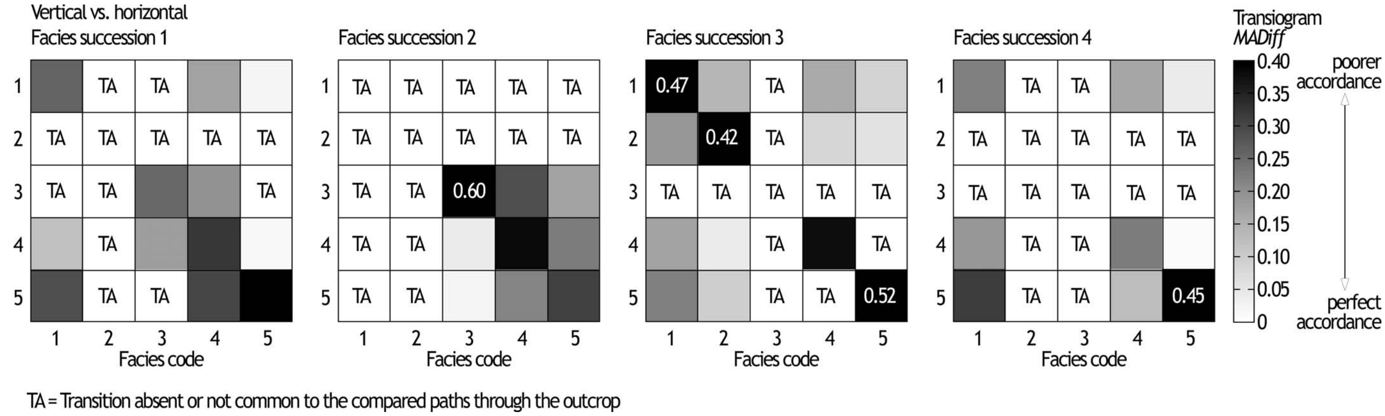

FIG. 7.—Matrices of mean absolute difference (*MADiff*) values which assess the degree of similarity between 1-D discrete-lag Markov-chain models developed for every permutation of facies pairings, by succession, for vertical sections vs. horizontal transects. For *MADiff* $>$ 0.40, values are written into the matrices. Facies codes are: 1 = peloidal wacke-mudstone, 2 = skeletal–foram grainstone, 3 = burrowed packstone, 4 = rudist packstone, and 5 = bivalve packstone.

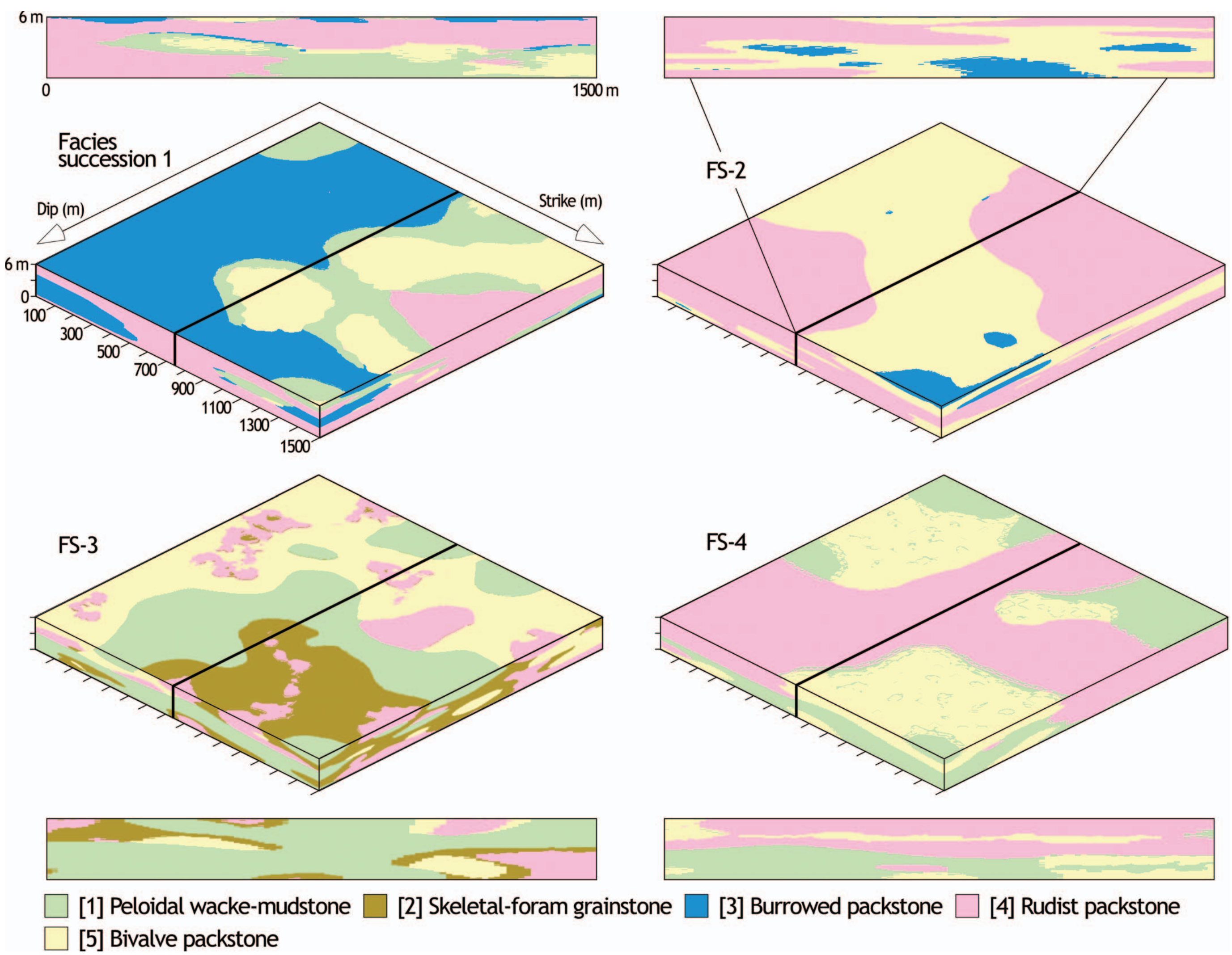

FIG. 8.—Output MRFS volumes for the four facies successions. These Markov models are conditioned solely using vertical facies transition probabilities and mean vertical and lateral extents as extracted from the outcrop panel. A dip-oriented slice through the center of each volume (heavy black line) is extracted to reveal the internal geometry of the simulation. Compared to the outcrop, the modeled facies associations are visually realistic.

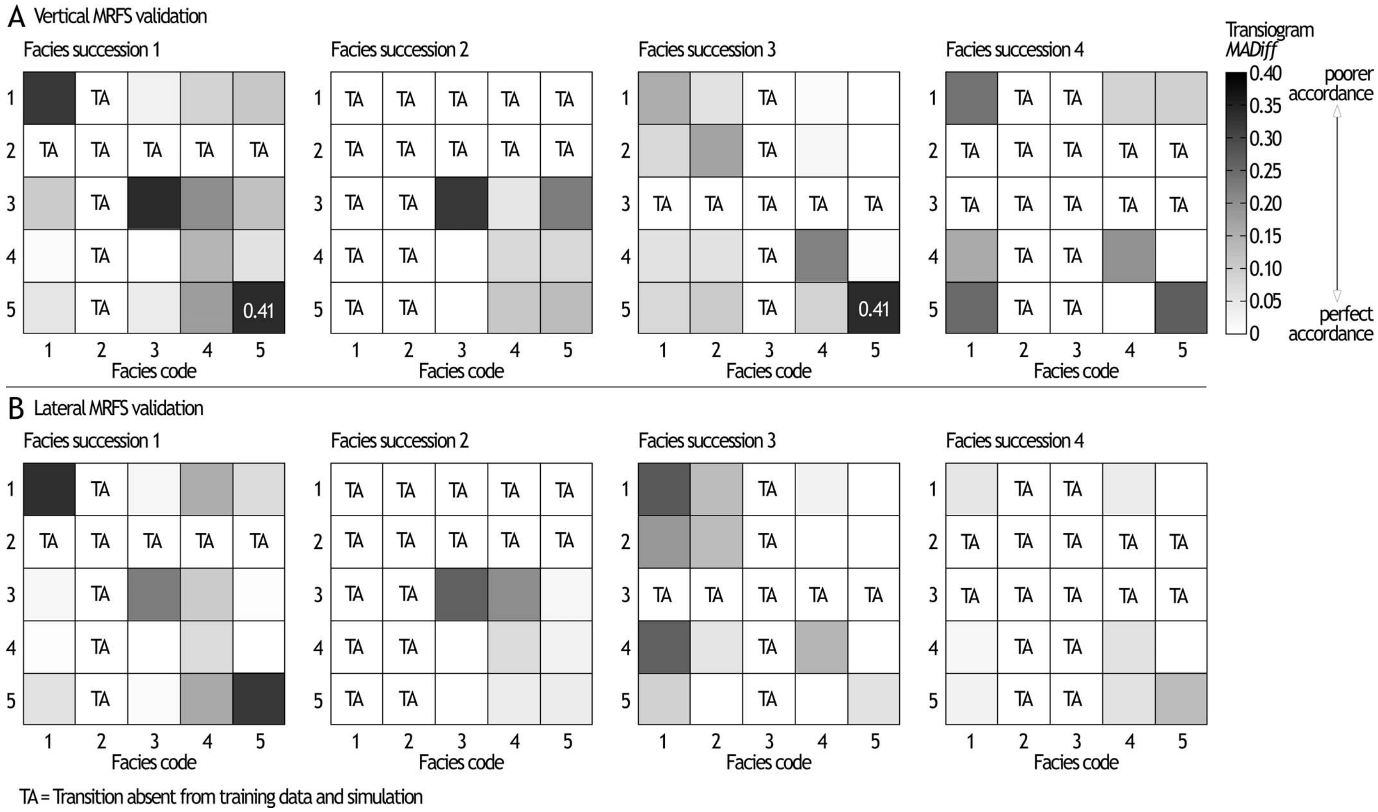

FIG. 9.—Matrices of mean absolute difference (*MADiff*) values assessing the degree of similarity between 1-D discrete-lag Markov-chain models developed in the **A)** vertical and **B)** lateral direction of the simulated volume, and the outcrop data used to condition it. Matrices are partitioned by succession. Darker shades of gray depict greater discordance than light and values of *MADiff* > 0.40 values are quoted. Facies codes are: 1 = peloidal wacke-mudstone, 2 = skeletal–foram grainstone, 3 = burrowed packstone, 4 = rudist packstone, and 5 = bivalve packstone.

($p = 0.05$). Lastly, the observations from Lewis Canyon were framed through the development of a proof-of-concept 3-D Markov random field simulation based upon Carle et al. (1998). The simulation was shown to be geologically plausible, returning a faithful representation of the medium within each succession, even given that it was conditioned using very sparse data; solely, vertical facies transitions and mean vertical and lateral extents which were harvested from outcrop. If applied to the search and extraction of hydrocarbons in carbonate rocks, the MRFS workflow can be considered capable of delivering considerable insight from relatively limited numbers of wells penetrating a deposit of interest. This simulation strategy promises to be powerful in the all-too-common situation where stratigraphic architecture is well constrained in the vertical from core but undersampled in the horizontal. Markov-inspired geostatistical models offer a probabilistic approach, grounded by fundamental geologic principles, to address this knowledge-gap.

ACKNOWLEDGMENTS

In writing this paper, we have benefited from productive Markov discussions with Bernhard Riegl, Rob Forkner, Erwin Adams, Peter Burgess, and Jim Jennings. The study was facilitated through access to skillfully interpreted exposures in Lewis Canyon provided by Charles Kerans and colleagues. Valuable reviews of our manuscript were delivered by Gene Rankey, Bruce Wilkinson, Klaas Verwer, and Wan Yang. We are grateful for their insight. This work was supported by Grant 4600005495 from Shell Int. E and P to Sam Purkis at the National Coral Reef Institute hosted by the NSU Oceanographic Center. Nuno Gracias was supported by the Spanish MCINN under the Ramon y Cajal program. This is NCRI publication 138.

REFERENCES

BOSENCE, D., PROCTER, E., AURELL, M., KAHLA, A.B., BOUDAGHER-FADEL, M., CASAGLIA, F., CIRILLI, S., MEHDIE, M., NIETO, L., REY, J., SCHERREIKS, R., SOUSSI, M., AND WALTHAM, D., 2009, A dominant tectonic signal is high-frequency, peritidal carbonate cycles? a regional analysis of Liassic platforms from western Tethys: Journal of Sedimentary Research, v. 79, p. 389–415.

CARLE, S.F., AND FOGG, G.E., 1997, Modeling spatial variability with one and multidimensional continuous-lag Markov chains: Mathematical Geology, v. 29, p. 891–918.

CARLE, S.F., LABOLLE, E.M., WEISSMANN, G.S., VANBROCKLIN, D., AND FOGG, G.E., 1998, Conditional simulation of hydrofacies architecture: a transition probability/Markov approach, *in* Fraser, G.S., and Davis, J.M., eds., Hydrogeologic Models of Sedimentary Aquifers: SEPM, Special Publication, Concepts in Hydrogeology and Environmental Geology, no. 1, p. 147–170.

DAVIS, J.C., 2002. Statistics and Data Analysis in Geology, Third Edition: New York, John Wiley and Sons, 637 p.

DOVETON, J.H., 1971, An application of Markov chain analysis to the Ayreshire coal measures succession: Scottish Journal of Geology, v. 7, p. 11–27.

DOVETON, J.H., 1994, Theory and application of vertical variability measures from Markov chain analysis, *in* Yarus, J.M., and Chamberlain, A.L., eds., Computer Applications in Geology 3: American Association of Petroleum Geologists, p. 55–64.

ELFEKI, A., AND DEKKING, M., 2001, A Markov chain model for subsurface characterization: theory and applications: Mathematical Geology, v. 33, p. 569–589.

ELFEKI, A., AND DEKKING, M., 2005, Modeling subsurface heterogeneity by coupled Markov chains: directional dependency, Walther's law and entropy: Geotechnical and Geological Engineering, v. 23, p. 721–756.

FULLMER, S., KACZMAREK, S.E., AND STEFFEN, K., 2010, Modern carbonate facies: moving from description to quantitative prediction [abstract], *in* Wood, L., Simo, T., and Rosen, N., eds., Seismic Imaging of Depositional and Geomorphic Systems, Program and Abstracts: 30th Annual Gulf Coast Section, SEPM Foundation, Bob F. Perkins Research Conference, Houston, Texas.

GOTELLI, N.J., AND ELLISON, A.M., 2004, A Primer of Ecological Statistics: Sunderland, Massachusetts, Sinauer Associates, 510 p.

Harris, P.M., and Vlaswinkel, B.M., 2008, Modern isolated carbonate platforms: templates for quantifying facies attributes of hydrocarbon reservoirs, *in* Lukasik, J., and Simo, T., eds., Controls on Carbonate Platform and Reef Development: SEPM, Special Publication 89, p. 323–341.
Harris, P.M., Ellis, J.M., and Purkis, S.J., 2010, Delineating and Quantifying Depositional Facies Patterns of Modern Carbonate Sand Deposits on Great Bahama Bank: SEPM, Short Course Notes, v. 54, p. 1–51, appendix p. 1–31, and 2 DVDs.
Harris, P.M., Purkis, S.J., and Ellis, J., 2011, Analyzing spatial patterns in modern carbonate sand bodies from Great Bahama Bank: Journal of Sedimentary Research, v. 81, p. 185–206.
Iosifescu, M., 1980. Finite Markov Processes and Their Applications: New York, John Wiley and Sons, 295 p.
Kemeny, J.G., and Snell, J.L., 1960. Finite Markov Chains: Berlin, Springer-Verlag, 224 p.
Kerans, C., 2002, Styles of rudist buildup development along the northern margin of the Maverick Basin, Pecos River Canyon, Southwest Texas: Gulf Coast Association of Geological Societies, Transactions, v. 52, p. 501–516.
Kerans, C., Fitchen, W., Zahm, L., and Kempter, K., 1995. High-frequency sequence framework of Cretaceous (Albian) carbonate ramp reservoir analog outcrops, Pecos River Canyon, northwestern Gulf of Mexico Basin: The University of Texas at Austin, Bureau of Economic Geology, Field Trip Guidebook, 105 p.
Krumbein, W.C., and Dacey, M.F., 1969, Markov chains and embedded Markov chains in geology: Mathematical Geology, v. 1, p. 79–96.
Lehmann, C.D., Osleger, A., and Montañez, I., 2000, Sequence stratigraphy of Lower Cretaceous (Barremian–Albian) carbonate platforms of northeastern Mexico: regional and global correlations: Journal of Sedimentary Research, v. 70, p. 373–391.
Lehrmann, D.J., and Rankey, E.C., 1999, Do meter-scale cycles exist? A statistical evaluation from vertical (1-D) and lateral (2-D) patterns in shallow-marine carbonates–siliciclastics of the "fall in" strata of the Capitan Reef, Seven Rivers Formation, Slaughter Canyon, New Mexico, *in* Saller, A.H., Harris, P.M., Kirkland, B.L., and Mazzullo, S.J., eds., Geologic Framework of the Capitan Reef: SEPM, Special Publication 65, p. 51–62.
Li, W., and Zhang, C., 2007, A random-path Markov chain algorithm for simulating categorical soil variables from random point samples: Soil Science Society of America, Journal, v. 71, p. 656–668.
Lin, C., and Harbaugh, J.W., 1984. Graphic display of two- and three-dimensional Markov computer models in geology: :New York, Van Nostrand Reinhold, 180 p.
Middleton, G.V., 1973, Johannes Walther's Law of the Correlation of Facies: Geological Society of America, Bulletin, v. 84, p. 979–988.
Papoulis, A., 1984. Probability, Random Variables, and Stochastic Processes, Second Edition: New York, McGraw-Hill, 852 p.
Parks, K.P., Bentley, L.R., and Crowe, A.S., 2000, Capturing geological realism in stochastic simulations of rock systems with Markov statistics and simulated annealing: Journal of Sedimentary Research, v. 70, p. 803–813.
Politis, D.N., 1994, Markov chains in many dimensions: Advances in Applied Probability, v. 26, p. 756–774.
Powers, D.W., and Easterling, R.G., 1982, Improved methodology for using embedded Markov chains to describe cyclical sediments: Journal of Sedimentary Petrology, v. 52, p. 913–923.
Purkis, S.J., and Kohler, K.E., 2008, The role of topography in promoting fractal patchiness in a carbonate shelf landscape: Coral Reefs, v. 27, p. 977–989.
Purkis, S.J., Riegl, B., and Andréfouët, S., 2005, Remote sensing of geomorphology and facies patterns on a modern carbonate ramp (Arabian Gulf, Dubai, U.A.E.): Journal of Sedimentary Research, v. 75, p. 861–876.
Purkis, S.J., Kohler, K.E., Riegl, B.M., and Rohmann, S.O., 2007, The statistics of natural shapes in modern coral reef landscapes: Journal of Geology, v. 115, p. 493–508.
Purkis, S.J., Rowlands, G.P., Riegl, B.M., and Renaud, P.G., 2010, The paradox of tropical karst morphology in the coral reefs of the arid Middle East: Geology, v. 38, p. 227–230.
Rankey, E.C., 2002, Spatial patterns of sediment accumulation on a Holocene carbonate flat, northwest Andros Island, Bahamas: Journal of Sedimentary Research, v. 72, p. 591–601.
Riegl, B., and Purkis, S.J., 2009, Markov models for linking facies in space and time (Arabian Gulf, Miocene Paratethys), *in* Swart, P., and McKenzie, J., eds., Perspectives in Sedimentary Geology: A Tribute to the Career of Robert Ginsburg: International Association of Sedimentologists, Special Publication 41, p. 337–360.
Roberts, F.S., 1976. Discrete Mathematical Models: Englewood Cliffs, N.J., Prentice-Hall, 559 p.
Rose, P.R., 1972. Edwards Group, Surface and Subsurface, Central Texas: The University of Texas at Austin, Bureau of Economic Geology, Report of Investigations 74, 198 p.
Salomão, M.C., and Remacre, A.Z., 2001, The use of discrete Markov random fields in reservoir characterisation: Journal of Petroleum Science and Engineering, v. 32, p. 257–264.
Scott, R.W., 1990, Models and Stratigraphy of Mid Cretaceous Reef Communities, Gulf of Mexico: SEPM, Concepts in Sedimentology and Paleontology, v. 2, 102 p.
Switzer, P., 1965, A random set process in the plane with a Markovian property: Annals of Mathematical Statistics, v. 36, p. 1859–1863.
Verwer, K., Della Porta, G., Merino-Tomé, O., and Kenter, J.A.M., 2009, Controls and predictability of carbonate facies architecture in a Lower Jurassic three-dimensional barrier-shoal complex (Djebel Bou Dahar, High Atlas, Morocco): Sedimentology, v. 56, p. 1801–1831.
Walther, J., 1894. Einleitung in die Geologie als historische Wissenschaft: Jena, Verlag von Gustav Fisher, 3 vols., 1055 p.
Weissmann, G.S., and Fogg, G.E., 1999, Multi-scale alluvial fan heterogeneity modeled with transition probability geostatistics in a sequence stratigraphic framework: Journal of Hydrology, v. 226, p. 48–65.
Weissmann, G.S., Carle, S.F., and Fogg, G.E., 1999, Three dimensional hydrofacies modeling based on soil surveys and transition probability geostatistics: Water Resources Research, v. 35, p. 1761–1770.
Wilkinson, B.H., Drummond, C.N., Rothman, E.D., and Diedrich, N.W., 1997, Stratal order in peritidal carbonate sequences: Journal of Sedimentary Research, v. 67, p. 1068–1082.

Received 4 January 2011; accepted 28 November 2011.